Arch. Min. Sci. **70** (2025), 3, 525-556

Electronic version (in color) of this paper is available: http://mining.archives.pl

DOI: https://doi.org/10.24425/ams.2025.156297

VANCHO ADJISKI[1*], VÁCLAV ZUBÍČEK[2]

INTEGRATED ENVIRONMENTAL IMPACT ASSESSMENT OF THE SASA TAILING DAM FAILURE USING REMOTE SENSING TECHNIQUES

Failures of tailings dams represent a critical environmental hazard, releasing mining by-products that cause long-term damage to nearby ecosystems. This research presents a detailed analysis using remote sensing techniques of the 2003 Sasa tailing dam disaster in North Macedonia. By utilising Landsat 5 imagery and Google Earth Engine (GEE), multiple spectral indices-including Normalised Difference Vegetation Index (NDVI), Normalised Difference Moisture Index (NDMI), Normalised Difference Water Index (NDWI), Modified NDWI (MNDWI), and a turbidity proxy-were integrated to examine the immediate and spatial impacts on vegetation health, soil moisture, water presence, and sediment levels.

The findings indicated that the degree of ecological fluctuation of the river path was high in terms of vegetation stress, changes in soil moisture, water pooling, and turbidity.

These effects showed spatial gradients, with the impact reducing further from the contamination pathway, forming distinct zones of influence. Some areas at intermediate distances showed anomalous disturbances, combining sediment and hydrological changes that obstruct vegetation recovery. Pixel-level, buffer-based, and zone-based analyses, with Z-scores and correlation studies, revealed complexity in post-disaster landscapes. Importantly, the weak correlation with topographic features suggested localised conditions, rather than broad gradients, governed short-term ecological recovery.

These results provide valuable insight for policymakers, demonstrating how multi-index and multi-scale approaches are necessary to capture the varied ecosystem responses to tailings dam failures. This study offers a framework for other disaster sites and promotes better-targeted remediation, informed disaster planning, and sustainable management of post-mining landscapes in a rapidly changing global context.

Keywords: Tailings dam failure; Remote sensing; Environmental impact assessment; Multi-index analysis; Mining-related disasters

[1] FACULTY OF NATURAL AND TECHNICAL SCIENCES, GOCE DELCEV UNIVERSITY, STIP, NORTH MACEDONIA
[2] DEPARTMENT OF MINING ENGINEERING AND SAFETY, VSB – TUO, OSTRAVA PORUBA, CZECH REPUBLIC

* Corresponding author: vanco.adziski@ugd.edu.mk

1. Introduction

Failure of tailings dams, which are structures designed to hold onto mining byproducts, can pose significant risks to environmental integrity, public health, and economic stability [1-5]. Such disasters can be very devastating, as evidenced by the Mariana (2015) and Brumadinho (2019) dam collapses in Brazil. They result in the release of hazardous substances, continuous pollution of river basins, disruption of ecosystems, and loss of human lives [1,6-8]. These events have created a global pressure to intensify, be proactive, and use scientifically grounded methods to monitor, assess, and mitigate the impacts of tailings dam failures [9-12]. Remote sensing has come into focus for post-disaster assessment because of its capacity to deliver quick, extensive, and consistent data over space and time [13-16]. A range of satellite-based methods, including optical imagery, Synthetic Aperture Radar (SAR), multispectral indices, and advanced analytical techniques, have been employed to monitor changes in vegetation health, soil moisture, sediment transport, and water quality after dam failures [17-19]. Notable studies have used indices like NDVI, NDMI, NDWI, MNDWI, and turbidity proxies to map environmental degradation and track recovery trajectories [9,20]. For instance, research on the Doce and Paraopeba Rivers in Brazil demonstrates how multi-sensor data can capture vegetation loss, sediment buildup, and shifts in hydrological regimes [4].

Although progress has been made, significant gaps appear. In many evaluations, single-indicator metrics are utilised, which risk overlooking the interconnected nature of ecosystem responses [21]. In addition, much of the available research emphasises widely recognised disaster sites, leaving regions like Eastern Europe and the Balkans underrepresented. More complex integrative techniques that involve several spectral indices are critically needed, especially in areas with limited data and research coverage, in order to give a more complete overview of post-disaster ecosystems. To address these gaps, this study adopted a multi-index remote sensing strategy that examines the environmental impact of the 2003 Sasa tailing dam disaster in North Macedonia.

While our focus is on the Sasa tailing dam incident, it's crucial to emphasise that the multi-index approach introduced here is designed to be broadly applicable to tailings dam failures worldwide, including areas with limited field data or less-documented events. By combining multiple spectral indices, practitioners can achieve rapid and robust environmental assessments, making this framework adaptable to other post-mining disasters or underrepresented regions.

We examine changes in vegetation health, soil moisture, water presence, and water clarity along the river's path and in the buffer zones around it by combining NDVI, NDMI, NDWI, MNDWI, and a turbidity proxy. This approach not only documents the spatial extent and severity of damage but also identifies patterns of resilience and vulnerability in the affected landscape.

Such findings make this study useful for understanding the implications of tailings dam failures and bring attention to an overlooked event in a neglected area. The conclusions can help the implementation of remediation activities, shape the disaster policies and contribute to the development of international regulatory frameworks for preventing mining-induced environmental disasters.

2. Sasa tailing dam failure: event description

The Sasa mine, in the vicinity of Makedonska Kamenica, North Macedonia, is an underground mine of lead and zinc that uses flotation methods to separate valuable minerals from the

ore (Fig. 1). Residual materials remaining after processing are called tailings, and they are stored in specialised impoundments to prevent their discharge into the environment. At the Sasa mine, this storage system consisted of a downstream sand dam built in stages and a settlement pond formed by the natural sedimentation of cyclone-generated sludge. Over time, this configuration was supposed to control the constant influx of tailings and allow fine particles to settle, reducing threats to downstream ecosystems.

Fig. 1. Location of the Sasa tailing dam failure in R. N. Macedonia

On August 30, 2003, a severe weather event exposed flaws in this system. Intense rainfall obstructed a major drainage component, "collector 6," preventing runoff from entering the intended diversion tunnel [22]. This resulted in water buildup within the tailings site at levels surpassing the initial design specifications. This excess water weakened the structure of the drainage system and led to a catastrophic drainage structure failure that released about 150,000 m^3 of tailings and processed water into the environment. This loosened material flowed downstream along the Sasa River, reaching the Kalimanci accumulation and spreading contamination over a broad and ecologically sensitive region [23]. At the failure point, a large crater over 100 meters in diameter emerged within the tailings site, dramatically changing the landscape and emphasising the scale of the event (Fig. 2).

Satellite images recorded the site prior to and following the failure (Fig. 2a). Images from August 16, 2003, show a stable tailings impoundment incorporated into the surrounding topography. In contrast, post-event imagery from 17 September 2003, enhanced with NDWI to highlight water presence, reveals a dramatically altered site: a large crater interrupts the terrain, and shifts in spectral signatures indicate changes in water content and surface conditions. Ground-level photographs (Fig. 2b) corroborate these satellite findings, providing a closer look at the crater's scale and complexity. Combined, these visuals demonstrate the breach's destructive morphological and environmental consequences.

In the aftermath, the Government of North Macedonia effectively staged a response. Emergency intervention measures, including water quality evaluation, removal of sediment and silt in the riverbeds, were implemented, and an additional overflow canal was built to restore hydrological balance. Other long-term plan measures were to repair sections of the diversion tunnel that were destroyed by the incident, as well as to suggest structural improvements to increase resilience. Some primary interventions, including the repair of the gallery tunnel and completely backfilling

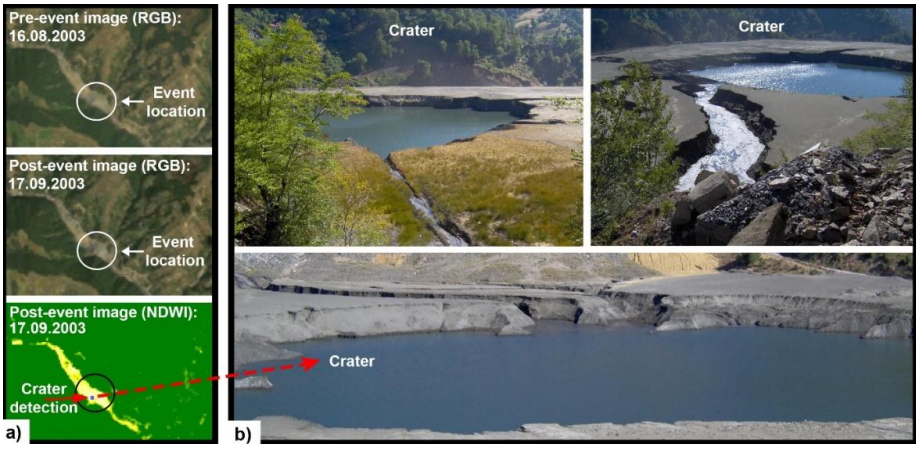

Fig. 2. Multi-Perspective analysis of the Sasa tailing dam failure: (a) Satellite imagery before and after the event (Landsat 5); (b) Ground-level photographs of the crater

the crater, had remained uncompleted due to a change of mine ownership and the alteration of operation strategies. These partial remediation measures, and the economic exploitation value of the mine, have made the tailings site a persistent problem. Monitoring systems, including piezometric surveillance to track groundwater pressure, are essential to ensure the stability of the dam, especially with the decision to resume production and construct a new tailings storage facility downstream. The Sasa tailings dam failure has both implications as a lesson and a valuable case study. It shows the complex relationships for environmental factors, engineering decisions and socio-economic aspects that influence risk management in the mining industry. The post-event images shown in Fig. 3 illustrate the severe environmental degradation along the river path and surrounding areas, which underline the need for effective monitoring and management strategies.

Fig. 3. Post-event impacts on the river path and surrounding environment following the Sasa tailing dam incident

3. Methodology

In this study, we use a multi-index remote sensing approach to assess the adverse effects of the 2003 Sasa tailing dam failure. We aimed to identify geographic gradients of impact and expose underlying ecological processes by combining spectral indices sensitive to vegetation health, moisture dynamics, and water clarity.

All investigations were carried out using GEE, which has high computational performance, multitemporal image collections, and a wide range of analysis tools [24,25]. A complete methodology flowchart, shown in Fig. 4, depicts the step-by-step approach, from defining the study region and preparing data to conducting spatial analyses and analysing the results.

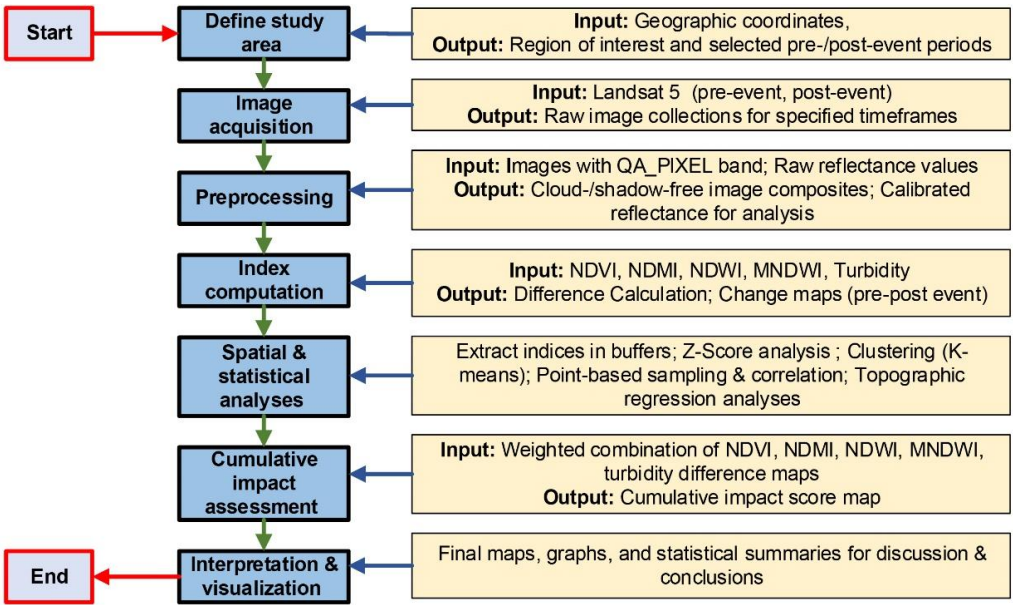

Fig. 4. Overview of the methodology flowchart for environmental impact assessment used in this study

3.1. Study area and period of analysis

The region of interest (ROI) is located in Makedonska Kamenica, North Macedonia, and it encompasses the Sasa mine tailings dam, downstream river channel and adjacent terrain (Fig. 5a). Using geometry tools in GEE, the spatial extent was defined to include the primary flow path of the tailings as well as areas potentially affected by secondary deposition.

Two specific dates were selected – 16 August 2003 (pre-event) and 17 September 2003 (post-event) – to capture the immediate ecological impacts of the tailings dam failure. The event occurred on 30 August 2003, and governmental reports indicate that cleanup and remediation activities began soon afterwards. By using images only a month apart, we minimise confounding factors from seasonal changes in vegetation, temperature, and moisture while avoiding interference

from remediation efforts. Additionally, historical field measurements and detailed environmental records for this period are scarce, largely due to the socio-political conditions in 2003 that limited public transparency and controlled information dissemination. Consequently, this approach highlights the value of remote sensing in retrospectively examining underdocumented incidents, enabling objective environmental assessments despite data constraints.

3.2. Data sources & preprocessing

3.2.1. Satellite Imagery

Landsat 5 Tier 1 Surface Reflectance (Collection 2) was used for this study due to its historical continuity, radiometric consistency, and appropriate spatial resolution of 30 m. The indices which were normally used to estimate vegetation health, soil moisture, and water quality were made possible by the multispectral capabilities of Landsat 5 [26].

3.2.2. Image selection and cloud masking

Only candidate images with low cloud coverage were filtered by using metadata within these temporal windows. A cloud masking algorithm was applied to the QA_PIXEL band, excluding pixels that were tainted by clouds, shadows, or snow/ice. This preprocessing procedure enhanced the credibility of the data by eliminating such features in the atmosphere and the surface that distort the calculation of the indices [27].

3.2.3. Radiometric calibration and scaling

All reflectance measurements were normalised using Landsat 5 Collection 2 scaling factors and offsets. These modifications guaranteed that reflectance data were consistent over time and places, allowing for direct comparisons between pre- and post-event circumstances [28].

3.3. Computation of spectral indices

A set of spectral indices was selected based on their demonstrated utility in environmental disaster assessments and their complementary sensitivities [29-33]:

- Normalised Difference Vegetation Index (NDVI):

$$NDVI = \frac{NIR - RED}{NIR + RED} \tag{1}$$

- Normalised Difference Moisture Index (NDMI):

$$NDMI = \frac{NIR - SWIR1}{NIR + SWIR1} \tag{2}$$

- Normalised Difference Water Index (NDWI) :

$$NDWI = \frac{GREEN - NIR}{GREEN + NIR} \tag{3}$$

- Modified NDWI (MNDWI):

$$MNDWI = \frac{GREEN - SWIR1}{GREEN + SWIR1} \tag{4}$$

- Turbidity Proxy:

$$Turbidity\ Proxy = SWIR1 - GREEN \tag{5}$$

where:

NIR (Near Infrared Reflectance) – Sensitive to vegetation biomass and vigor;
RED (Red Reflectance) – Absorbed strongly by chlorophyll during photosynthesis, indicating vegetation health;
GREEN (Green Reflectance) – Represents the visible spectrum sensitive to vegetation and water presence;
SWIR1 (Shortwave Infrared Reflectance Band 1) – Sensitive to soil moisture and water content.

Descriptions and applications of indices:

- NDVI: Quantifies vegetation health and productivity. Pre- and post-event comparisons highlight vegetation stress associated with sediment deposition or contamination (Fig. 5b).
- NDMI: Measures vegetation and soil moisture. Changes indicate altered hydrological conditions, such as soil saturation or drying after the tailings release (Fig. 5c).
- NDWI and MNDWI: Assess surface water presence and moisture retention. NDWI and MNDWI values elucidate whether tailings deposition influenced surface water distribution or moisture retention patterns (Fig. 5d,e).
- Turbidity proxy: Captures sediment loads and water clarity. Higher turbidity readings indicate increasing sediment loads and decreased water clarity, which are crucial for understanding the distribution of contamination and its impact on the environment (Fig. 5f).

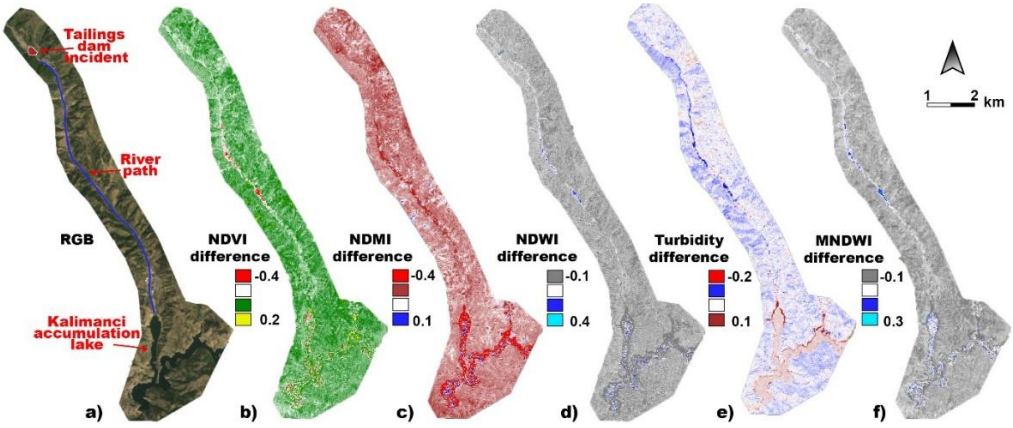

Fig. 5. Spatial visualisation of environmental indices differences pre- and post-event across the Sasa tailing dam impact area: (a) RGB Imagery; (b) NDVI difference; (c) NDMI difference; (d) NDWI difference; (e) Turbidity difference; (f) MNDWI difference

All indices were calculated for both pre- and post-event periods (Eqs. (1)-(5)). Difference maps (post-event minus pre-event) were generated to visualise the magnitude and direction of change across each environmental metric.

3.4. Spatial and statistical analyses

3.4.1. Buffer zones and gradient analyses

To determine the spatial extent and intensity of impacts, we marked the river course and buffer zones were created depicting 10 m, 25 m and 50 m from the river channel. Such barriers facilitated the smooth conduct of a gradient analysis, which assesses the degree of variations in environmental conditions as one gets farther away from the contamination source. The mean value and distribution of each index were calculated within each buffer zone to differentiate regional and scattered effects.

3.4.2. Z-Score analysis

A Z-score technique was adopted to estimate the statistical extent of the observed changes, typically in the form of vegetation health (NDVI) (Eq. (6)) [34,35]. The pre-event condition was observed, where the mean (μ) and standard deviation (σ) were used as a baseline to standardise post-event NDVI readings. Differentiation of significant abnormalities by a certain threshold level proved useful in isolating areas of high ecological stress. The Z-score was calculated using the formula:

$$Z = \frac{X - \mu}{\delta} \tag{6}$$

where:

X – observed NDVI value (post-event);
μ – mean of pre-event NDVI values;
δ – standard deviation of pre-event NDVI values.

3.4.3. Clustering and anomaly detection

K-means clustering was applied to pixels sampled from the river path and buffer zones (Eq. (7)) [36,37]. Thus, we differentiated the environmental ‘signatures‘ of classes by clustering pixels based on NDVI, NDMI, NDWI, MNDWI, and turbidity. These clusters allowed for the interpretation of intricate relationships and patterns, for instance, regions where high moisture and vegetation stress co-occurred, or zones with elevated turbidity and reduced vegetation. The K-means algorithm partitions n data points into k clusters by minimising the within-cluster variance (WCV), which is calculated as:

$$WCV = \sum_{i=1}^{k} \sum_{x \in C_i} \| x - \mu_i \|^2 \tag{7}$$

where:

k – number of clusters;
C_i – the i-th cluster;

x – a data point in cluster C_i;
μ_i – the centroid of cluster C_i.

3.4.4. Point-based sampling and correlation analyses

A series of point samples done along the river corridor and in affected communities further confirmed the existence of fine-scale heterogeneity. For further analysis of the relationship of indices to each other, we performed Pearson correlation analysis on the index values obtained at these points (Eq. (8)) [38,39]. For instance, we tested whether the zones with high NDWI also had low NDVI, signifying flooding or sediment-associated waters that negatively affected vegetative health. The Pearson correlation coefficient r was calculated as:

$$r = \frac{\sum \left(X_i - \underline{X}\right)\left(Y_i - \underline{Y}\right)}{\sqrt{\sum \left(X_i - \underline{X}\right)^2 \sum \left(Y_i - \underline{Y}\right)^2}} \tag{8}$$

where:
X_i – value of the first variable (e.g., NDWI);
Y_i – value of the second variable (e.g., NDVI);
$\underline{X}$ – mean of the first variable;
$\underline{Y}$ – mean of the second variable.

3.4.5. Topographic factors and regression analysis

Simple linear regression was used to observe if topographic features like elevation or distance downstream impacted the observed environmental changes (Eq. (9)) [40-42]. These analyses were more exploratory, but they provided the tools we need to determine if the patterns of damage are a result of local contamination events or if it is more influenced by broader landscape features. The regression model is expressed as:

$$Y = \beta_0 + \beta_1 X + \varepsilon \tag{9}$$

where:
Y – dependent variable (e.g., NDVI, NDMI, or Turbidity differences);
X – independent variable (e.g., elevation or distance downstream);
β_0 – intercept, representing the baseline value of Y when $X = 0$;
β_1 – Sslope, representing the rate of change in Y with respect to X;
ε – error term, accounting for variations not explained by the model.

3.4.6. Cumulative impact assessment

The methodology incorporates multi-source information, such as remote sensing, statistical data, and machine learning approaches to establish the overall effects of the Sasa tailings dam failure. Specifically, the sampling was conducted inside three zones – Zone 1, Zone 2 and Zone 3 in GEE, obtaining pixel values of NDVI, NDMI, NDWI, MNDWI and turbidity in order to measure environmental disturbance.

Thus, the index weights were derived based on a Principal Component Analysis (PCA) in Python. Standardised indices were analysed, and weights were normalised from the contributions of the first principal component (PC1) [43,44]. These weights were used in GEE to compute a Cumulative Impact Score (CIS) (Equation 10) for each pixel, calculated as:

$$CIS = \sum \left(W_i + I_i \right) \tag{10}$$

where:

W_i – represents the weight of the i-th index derived from PCA,

I_i – represents the value of the i-th index.

The heat map of the cumulative impact scores was presented, with low impact in blue, moderate in white, and high impact in red. NDVI and NDWI differences were visualised with green-yellow and cyan-blue gradients. This approach identified locations of high-impact zones requiring intervention by combining vegetation health, moisture, and water quality data. Exported data included raw, normalised, and cumulative levels of scores for further analysis.

3.5. Sensitivity analysis of index differences

Multi-index methods reveal crucial spatial patterns of post-disaster effects between locations. It is essential to verify that the observed changes do not emerge due to random fluctuations or sensor noise. We conducted a statistical sensitivity analysis for our main indices – NDVI, NDMI, NDWI, MNDWI, and turbidity – focusing on a 10 m buffer zone along the river path. This zone was specifically chosen because it encompasses the most affected channel-adjacent areas, where the tailings spill was expected to have the most significant impact.

We used GEE to acquire pixel-wise pre-event and post-event index values exclusively from within the 10 m buffer zone. Each index was compiled into a paired dataset (i.e., the same pixel locations before and after the event) to enable paired statistical testing. The following steps were then applied:

1. Data cleaning: invalid or cloud-contaminated pixels were removed, ensuring that only clear, valid observations remained.
2. Difference calculation: for each pixel, the difference was computed as (post-event value) – (pre-event value).
3. Normality assessment: a Shapiro-Wilk test was used to assess whether the distribution of differences was normal.
4. Significance testing:
   - if the differences were normally distributed ($p > 0.05$), a paired t-test was used.
   - otherwise, a Wilcoxon signed-rank test was applied.

This procedure allowed us to validate the measured changes by establishing that statistically significant differences from zero helped rule out random noise as the primary cause of observed pattern trends. Consequently, this ensures that any subsequent ecological interpretations – including vegetation stress analysis, water pooling detection, and turbidity change monitoring – are based on robust statistical evidence rather than coincidental seasonal variations or sensor measurement errors.

4. Results and discussion

4.1. Environmental impact analysis of the Sasa tailing dam failure

The Sasa tailing dam collapse affected local vegetation health, soil moisture conditions, surface water, and turbidity to varying degrees within the region. To quantify the changes, we compared the spectral index differences before and after the event and found them to be elevated in the areas near the riverbed and in proximity to the spill, with the effects decreasing as one moves away from the primary contaminated pathway.

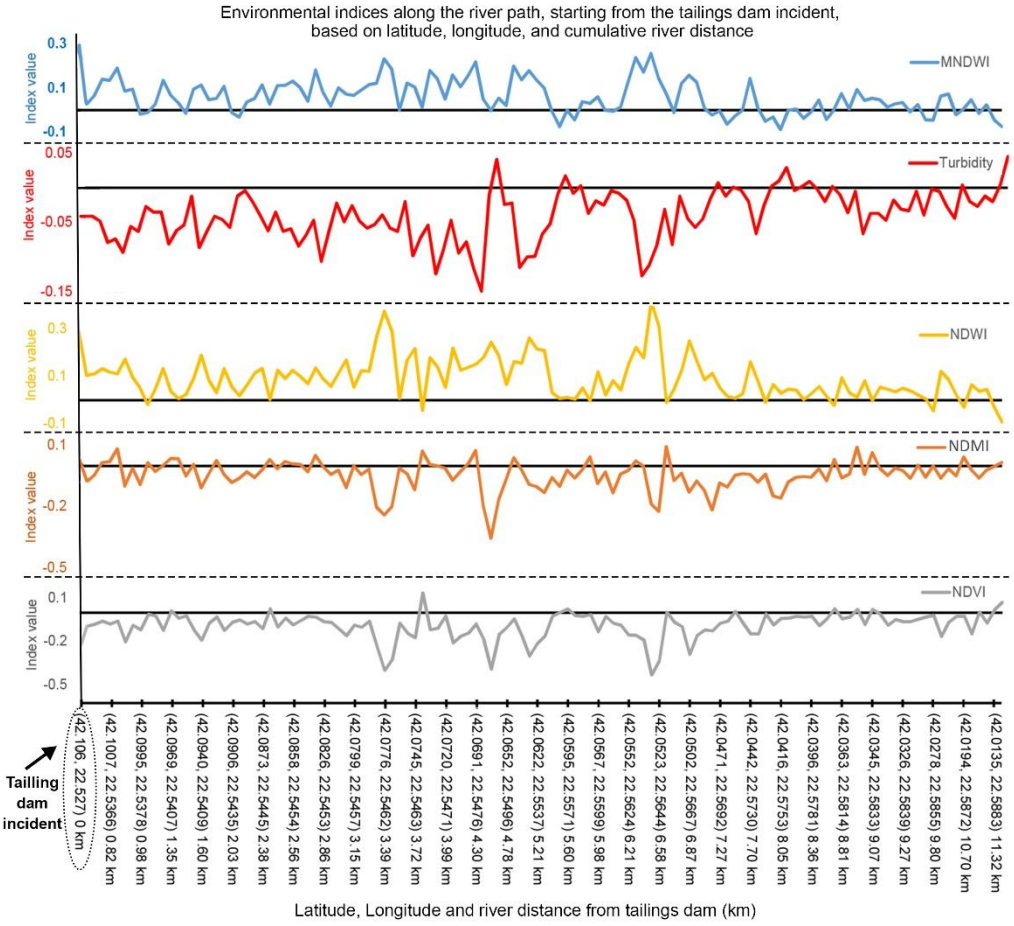

Fig. 6. Spatial variability of environmental index differences (pre- and post-event) along the river path, starting from the tailings dam incident. The x-axis displays geographic coordinates and cumulative river distance (km) from the tailings dam, representing the actual flow path of the material. Trends in NDVI, NDMI, NDWI, MNDWI, and turbidity highlight vegetation stress, moisture changes, surface water accumulation, and sediment transport following the tailings dam failure

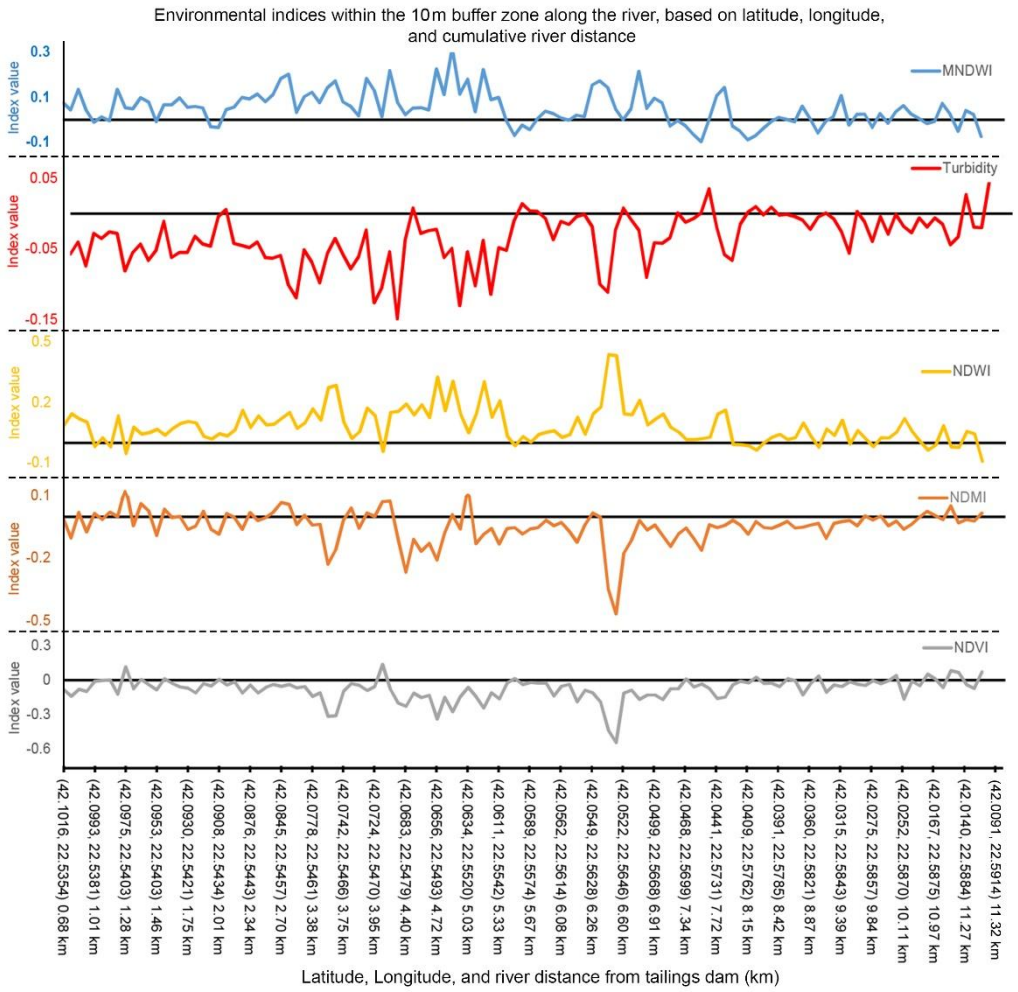

Fig. 7. Environmental index differences (pre- and post-event) within the 10 m buffer zone along the river corridor, incorporating geographic coordinates and cumulative river distance (km) from the tailings dam. Trends in NDVI, NDMI, NDWI, MNDWI, and turbidity highlight peripheral environmental changes beyond the immediate river channel

To improve spatial interpretation, Figs. 6 and 7 integrate both geographic coordinates and cumulative river distance from the tailings dam to visualise the environmental changes along the true flow path of the contaminated river corridor.

Further analysis of the data for changes in NDVI values before and after the event showed a decrease in vegetation density along the entire area of the river channel (beginning at the tailings dam incident site, as indicated in Fig. 6). Even in the worst-affected areas, the NDVI values declined to –0.43, which would suggest that vegetation was under serious stress or loss. This decline is most likely due to physical scouring, sediment deposition, and chemical contamina-

tion from the tailings material. In contrast, when comparing the graphs for the river path and the 10-meter buffer zone, the buffer zone exhibited a more moderate NDVI reduction, despite having a wider range from –0.5 to +0.1. This indicates that while some vegetation experienced stress, other areas showed resilience or were less directly impacted by tailings deposition (Fig. 7). These patterns highlight the necessity of fine-scale spatial analysis, as even short distances from the contaminated pathway resulted in very divergent ecological responses.

The changes in NDMI readings showed diverse patterns. Within the river path, NDMI ranged from –0.35 to +0.1, indicating both moisture deficits, possibly caused by vegetation die-off and subsequent changes in evapotranspiration, and localised moisture pooling in sediment-laden portions (Fig. 6). In the 10-meter buffer zone, NDMI changes were a little less pronounced, emphasising the localised nature of changed soil moisture levels (Fig. 7). The findings indicate that tailings-induced changes in surface roughness, soil structure, and infiltration rates were mostly limited to the immediate spill zone, altering moisture retention and availability in a heterogeneous way.

NDWI and MNDWI analyses demonstrated higher water retention and altered hydrological conditions throughout the river. The changes in NDWI readings climbed to 0.41, indicating the presence of either standing water or water-saturated soils, whereas MNDWI values remained around 0.25 in several parts (Fig. 6). The increase in these indices is most likely due to localised water pooling caused by tailings material impeding drainage or an abrupt change in the river channel shape. In contrast, the 10-meter buffer zone also exhibited changes, highlighting that the majority of hydrological disruptions occurred at the river interface (Fig. 7). Such localised water retention can have an impact on sediment transport, nitrogen cycling, and habitat suitability for aquatic and riverside species.

A turbidity proxy indicated elevated sediment loads and reduced water clarity along the immediate river path. Peaks in turbidity up to 0.05 were observed, reflecting the influx of fine-grained tailings into the water column (Fig. 6). Within the 10-meter buffer, turbidity increases were modest, again suggesting a tight spatial coupling between the failure site and its most intense environmental effects (Fig. 7). Presumably, the sediment settled out of the water column, but the increased turbidity represented a key disturbance to aquatic ecosystems and potential stress for downstream water users.

4.1.1. Synthesis of impacts

Overall, the integrated analysis of NDVI, NDMI, NDWI, MNDWI, and turbidity proved that the clear spatial pattern of environmental consequences gradually extends from the Sasa tailing dam failure. The river corridor experienced the most significant and immediate alterations: vegetation damage, shifts in soil moisture balance, increased surface water pooling, and elevated turbidity. In contrast, even a relatively short lateral distance from the channel conferred measurable buffering effects, resulting in comparatively milder environmental changes. These findings highlight the importance of multi-index remote sensing approaches, which can detect and unravel overlapping processes-such as sedimentation, contamination, and altered hydrology-that shape post-disaster landscapes.

The findings from our study about the 2003 Sasa tailing dam failure can be contextualised by comparing them with other remote sensing analyses of tailings dam disasters, in particular Mariana (2015) and Brumadinho (2019) in Brazil.

Researchers utilised satellite data to find substantial vegetation index decreases, which showed broad-scale vegetation destruction throughout affected areas during the Mariana disaster

[6]. Similarly, analyses of land cover variations based on the Brumadinho incident showed how the disaster zone experienced substantial forest loss [5,11].

Our results show comparable patterns. The satellite-derived vegetation indices NDVI and NDMI showed statistically significant reductions at the river corridor and adjacent buffer zones that corresponded with tailings deposits stress effects. Research outcomes about Brazilian disasters support the reliability and widespread use of remote sensing techniques for measuring tailings dam failure environmental impacts.

4.2. Comprehensive analysis of mean values for environmental indices along the river path and buffer zones

Following the pixel-level observations detailed in the preceding section, a more comprehensive examination of average index differences before and after the event was conducted to figure out how the event's effects diminish or persist at farther distances from the river corridor. By examining mean pre-to-post-event changes in NDVI, NDMI, NDWI, turbidity and MNDWI across the river path and two buffer zones (25 m and 50 m), we gained insights into the spatial distribution of environmental stressors induced by the tailings dam failure.

Fig. 8 illustrates the mean NDVI differences, which showed a distinct gradient of influence. Along the river path, the mean NDVI dropped by approximately –0.078, which indicates a highly significant vegetation loss in the investigated area where the deposition of the tailings and changes in the hydrological conditions had been more significant. At 25 meters from the river, the mean NDVI drop reduced to around –0.071, and by 50 meters, it decreased further to –0.054. This pattern suggests that while vegetation stress was acute at the river's edge, it progressively decreased with distance, indicating that contamination effects were spatially constrained and did not fully propagate into more distant terrestrial habitats.

Mean NDMI values exhibited a similar pattern of change with relatively low change in estimates along the river path with a value of –0.047 (Fig. 8). At 25 and 50 meters, NDMI decreases were slightly smaller (–0.042 and –0.04, respectively), indicating that soil moisture anomalies caused by tailings release were more concentrated along the river channel. Although moisture conditions remained affected at some distance, the signal diminished as one moved away from the point of maximum impact.

While vegetation and moisture indices declined, water-related metrics showed sharp increases near the river and gradually weakened in the buffer zones. In the river path, NDWI increased by approximately +0.082, representing an increase due to accumulation or saturation by tailings material that obstructs usual drainage (Fig. 8). At 25 m, it was still higher at +0.075, and at 50 m it was slightly lower at +0.065, which requires a combination of the hydrological area of influence of the spill to exceed just the channel width. Likewise, the MNDWI values increased near the river channel (+0.052) and declined gradually to 25m (+0.045) and 50m (+0.027). These outcomes combined suggest that alterations in hydrological conditions were more enduring and extended somewhat beyond the spill course, which may influence local groundwater recharge, vegetation-water relations, and soil characteristics.

Turbidity showed a noticeable decrease along the river path, with a mean difference of –0.035, likely due to sedimentation and settling of tailings materials after the initial disturbance (Fig. 8). This reduction was a little less pronounced in the 25 m (–0.028) and 50 m (–0.022) buffer zones.

4.2.1. Synthesis of spatial patterns

Fig. 8 illustrates how the mean differences in environmental indices vary across the river channel and buffer zones. Vegetation stress and soil moisture deficits were most pronounced at the river's edge and decreased with distance, reflecting the importance of proximity to the contamination source. In contrast, the results reflected the changes in the hydrological condition by demonstrating the effects of an increase in NDWI and MNDWI values that moved deeper into the buffer zones, indicating that changes in water dynamics have impacts over a wider spatial extent than vegetation loss. Turbidity, which had been elevated at some of the sampling sites, also seemed to decrease, suggesting that the disturbance may be of short duration or as a result of efficient sedimentation downstream.

Overall, this multi-scale, averaged analysis confirms a pattern observed at the pixel level: the tailings dam failure provided its most substantial ecological impact along the first section of the river. However, some processes, mostly regarding the presence of the surface water features, radiate out into the surrounding environment. These results suggest the need for intervention strategies and monitoring that do not concentrate on the areas of plainly visible and most severe impacts. It may, though, extend to adjacent regions where alterations in hydrological patterns may have concealed significant environmental effects.

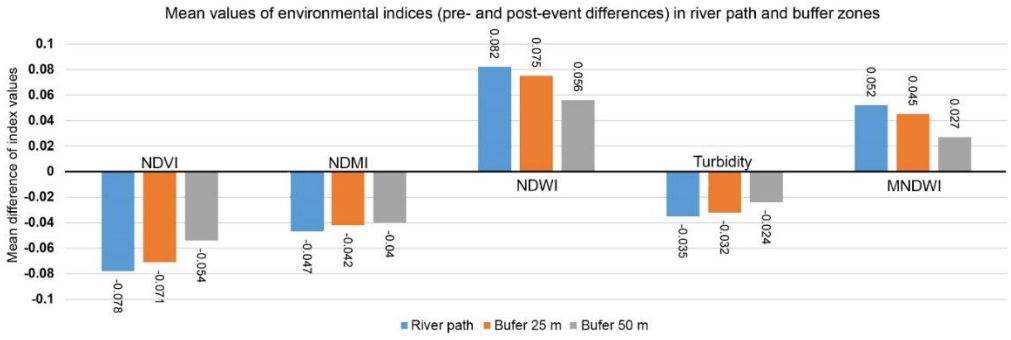

Fig. 8. Comparative analysis of mean environmental index differences (pre- and post-event): variations in NDVI, NDMI, NDWI, turbidity, and MNDWI across the river path and buffer zones at 25 m and 50 m

4.3. Comprehensive analysis of zone-based environmental impact post-Sasa tailing dam failure

To add a spatial dimension to the analysis of the environmental response, we divided this area into a zone-based analysis that categorised the affected area into three discrete segments downstream of the tailings dam incident. The field of assessment is divided as follows: Zone 1, which represents samples collected near the spill incident; Zone 2, which includes samples collected at a mid-distance from the spill incident; and Zone 3, which includes samples taken furthest downstream from the spill incident (Fig. 9a). To sample not only the mean conditions but also the variability and range of each of the environmental index differences (pre- and post-event): NDVI, NDMI, NDWI, Turbidity, and MNDWI over the affected areas in each zone, we used descriptive statistics, including the mean, median, maximum, minimum, and standard deviation (Fig. 9b).

b)

		max	min	mean	median	stdDev
NDVI	Zone 1	0.1168	-0.1912	-0.0179	-0.0133	0.0568
	Zone 2	0.1377	-0.2793	-0.0654	-0.0637	0.0729
	Zone 3	0.1083	-0.1477	-0.034	-0.0303	0.0506
NDMI	Zone 1	0.1434	-0.1082	-0.0068	-0.0044	0.0404
	Zone 2	0.0927	-0.2187	-0.0356	-0.0322	0.059
	Zone 3	0.0911	-0.155	-0.0461	-0.0509	0.0471
NDWI	Zone 1	0.1902	-0.0782	0.0332	0.0246	0.0528
	Zone 2	0.2401	-0.0562	0.0775	0.0712	0.0691
	Zone 3	0.1256	-0.0768	0.0286	0.0259	0.0375
Turbidity	Zone 1	0.0153	-0.0845	-0.0289	-0.028	0.0222
	Zone 2	0.0381	-0.1535	-0.0424	-0.0398	0.0428
	Zone 3	0.0237	-0.0664	-0.0106	-0.0091	0.0163
MNDWI	Zone 1	0.1509	-0.0507	0.0277	0.0232	0.0442
	Zone 2	0.274	-0.1499	0.0492	0.0356	0.0732
	Zone 3	0.1383	-0.0788	-0.0029	-0.0053	0.0393

Fig. 9. a) Visual representation of sampled zones; b) Summary of environmental indices differences across sampled zones

A more detailed breakdown of the results is presented in Fig. 9b, which illustrates that Zone 1 had a mean NDVI difference of –0.0179, with a range of –0.1912 to +0.1168. These moderate changes indicate that while vegetation stress was evident, it was not too dramatic. In Zone 2, the mean NDVI reduced to a lower level and was –0.0654, which ranged between –0.2793 and +0.1377, which may represent much more serious vegetation damage, and potentially a more heterogeneous response, possibly due to local site conditions and variable tailings deposition. Zone 3 indicated the mean NDVI of –0.034, and the variability was also lower in this zone, as compared to Zones 1 and 2. This pattern suggested a gradient in contamination and disturbance, with the maximum evident in Zone 2, where flow conditions may have favoured sediment accumulation, which decreased beyond this point.

The NDMI is an important indicator that supports the spatial amplification of the event's impact. Overall, according to the mean NDMI in Zone 1, it became evident that there were no significant, but also not negligible, modifications of moisture in this zone, with the mean equal to about –0.0068 (Fig. 9b). By comparison, Zone 2 showed a mean NDMI decline of –0.0356, suggestive of sizeable changes in the dynamics of soil moisture regulation and possibly consequences from tailings-induced near-surface crusts or infiltration modification. However, the mean reduction in NDMI for Zone 3 (–0.0461) was somewhat unexpected, as this zone is farther from the source. This might indicate residual downstream effects on soil moisture or delayed impacts of soil pollution as fine materials moved downstream. Fluctuations in the NDMI suggest that the local hydrological conditions might differ due to topographic or soil differences.

The calculation of NDWI for each evaluation demonstrated marked differences among the zones, explaining water retention or characteristics of channel shifts. The mean NDWI for Zone 1 was approximately 0.0332, which pointed toward slightly elevated surface moisture or saturated soil (Fig. 9b). Zone 2 had around 0.0775 of the NDWI value, implying that the mid-distance zone showed signs of considerable water pooling or retention. This could be due to changes in channel form or sedimentation barriers of some nature. The NDWI mean value in Zone 3 was around 0.0286, which showed that the change in water presence across the area is also visible. Such variations of NDWI indicated that the hydrological alteration was not limited to the area closer to the spill but was carrying changes in water ecosystems downstream.

Turbidity parameters were effective in expressing sediment transport and clarity. The mean turbidity in Zone 1 decreased slightly to a negative value (–0.0289), indicating that the spill may not have significantly increased sediment levels near the source and that sediment could have either settled quickly or dispersed in localised areas (Fig. 9b). There was a negative mean difference (–0.0424) observed in the turbidity difference in Zone 2, which indicated that the suspended sediments either precipitated or possibly got dispersed in some manner that led to an overall decrease in turbidity as compared to the state before the event. At Zone 3, the turbidity fluctuation was close to zero (–0.0106), signifying a slight long-term interruption of water clarity further downstream. These findings underscore that sediment transport processes transitioned rather rapidly from the immediate source area, thereby placing materials in complex patterns along the river corridor.

The patterns identified for MNDWI were similar to those identified for NDWI. Zone 1 had a rather small increase, of about 0.0277, Zone 2 had an even larger increase, of 0.0492, and Zone 3 reduced right to almost neutral conditions, –0.0029 (Fig. 9b). This means that water conditions in Zone 2 – dictated possibly by the morphology and flow of rivers -– fostered conditions that encouraged water retention. The slight shifts for Zone 3 can also be used to argue that even where hydrology alterations did go down to the downstream areas, they were not greatly intensive compared to upstream.

4.3.1. Synthesis of zone-based patterns

In Fig. 9a,b, as well as in the statistics associated with it, the different aspects of the phenomena that affected the formation of the post-disaster landscape are shown. Zone 2 emerged as a hotspot of change, showing pronounced decreases in NDVI, NDMI and turbidity alongside elevated NDWI and MNDWI. This means that Zone 2 may have been a transitional area where deposits, initially mobilised near the dam, encountered channel gradients or flow conditions conducive to sediment deposition and altered water dynamics. Zone 1, nearest to the source, did not have the most severe vegetation or moisture reduction-possibly due to partial remediation efforts or local channel formation that allowed the tailings to pass through quickly. Zone 3 showed less pronounced differences, suggesting that the contaminants had been diluted or settled over distance.

Such findings also suggest that environmental degradation of the Sasa tailing dam failure was both extensive and unevenly distributed, extending beyond the immediate spill site. Rather, it emerged as spatially varied ‘regions of influence’ that reflected local conditions, hydrological processes, and sediment transport regimes. Such a detailed understanding is essential for designing targeted mitigation strategies that address zone-specific challenges, whether that means stabilising soils, improving drainage, or restoring vegetation in the areas most affected by altered moisture and water conditions.

4.4. Comprehensive analysis of point-based sampling and correlation results

Although zone- and buffer-based assessments may provide strategic perspectives, a detailed, perhaps contextual study can add more specific insights into the different propagation of environmental change. To this end, we collected environmental indices at a number of fixed points in the river path (Fig. 10a). This point-based strategy enabled us to achieve high temporal density

in vegetation health, soil moisture, water presence, and turbidity, as these metrics can often show high variability at local, fine spatial scales because of topographical or microhabitat differences.

4.4.1. Localised patterns in environmental indices

Fig. 10b provides the statistical comparison of environmental index differences (pre- and post-event) of NDVI, NDMI, NDWI, turbidity and MNDWI at each sample point. Spatial patterns emerge even at this fine scale. For example, points near the tailings dam incident site generally depicted a higher negative shift on NDVI, which has an implication of a higher level of vegetation stress due to contamination and sediment load. As the sampling proceeded downstream, these changes were often less pronounced in degree, but not in a linear manner. Some points showed persistent moisture anomalies (e.g., NDMI variations) or water presence indicated by elevated NDWI and MNDWI values, suggesting localised pockets of water retention or hydrological alteration shaped by channel morphology, debris deposition, or sediment bar formation. Turbidity responses were equally variable.

Points with large increases in NDWI and MNDWI often are associated with smaller turbidity values, suggesting that, where water was pooling or in the process of saturating the soils, the sediments may have settled out, causing increased clarity. On the other hand, some points with relatively small changes in hydrological disruption might be characterised by relatively higher water turbidity, mainly attributed to finer sediment particles which took relatively longer time to settle in faster water currents.

4.4.2. Correlation analysis of environmental indices

To systematically interpret these relations, a Pearson correlation was carried out among the key indices (Fig. 10c). The resulting correlation coefficients offer preliminary insights into how changes in one environmental parameter might relate to another.

However, it is crucial to note that high correlations between remote sensing indices do not inherently imply causal or ecological relationships, as many indices are derived from overlapping spectral bands – particularly near-infrared (NIR) and shortwave infrared (SWIR) – which can mathematically bias the results. Therefore, the following correlations are interpreted as indicative spatial patterns rather than definitive biophysical linkages.

NDVI vs. NDWI: A strong negative correlation ($r = –0.9742$) indicates that areas with higher post-event water presence (NDWI) tended to experience more pronounced declines in vegetation health (NDVI). This relationship indicates that water pooling may have formed due to sediment buildup, creating conditions unsuitable for plant growth by enveloping roots or introducing contaminants that hindered their growth. This relationship specifies that water pooling formed perhaps because of sediment buildup, creating conditions that were unsuitable for plant growth through enveloping roots or contaminants that prevented them from growing.

NDMI vs. MNDWI: A comparatively negative correlation ($r = –0.3519$) also maintains differentiation between soil moisture (NDMI) and modified water index (MNDWI). Since both indices are related to moisture conditions, the negative correlation might be due to variation in the type or location of the moisture that is detected. For example, MNDWI can detect standing water or saturated soil surfaces. Meanwhile, NDMI, combining information from vegetation and soil, may more likely be affected by sub-surface moisture availability or vegetation interactions with water.

NDWI vs. Turbidity: A moderate positive correlation ($r = 0.5701$) shows that the areas that had a relatively high-water presence were also associated with relatively high levels of turbidity, at least at the initial stage. A distribution pattern like this could be attributed to continuous transport of sediments in the water body, and these pooling zones act as containers for the suspended particles. However, such particles may sink with time, thereby changing turbidity patterns as well. The given moderate level of correlation indicates that the variables of hydrological conditions and sediment load are closely linked but not strictly proportional.

NDMI vs. NDWI: A relatively strong negative correlation ($r = –0.7033$) indicates that increased values of surface water (NDWI) corresponded to reduced values of soil moisture (NDMI). Pooled water can restrict infiltration through different layers of the soil or make conditions of the area unsuitable for vegetation to control moisture. Such an inverse relationship could arise if the water accumulation disrupts the regular cycling of moisture in the soil affecting compaction of soils or infiltration rates.

MNDWI vs. Turbidity: A stronger negative correlation is apparent ($r = –0.8242$), implying that greater water clarity (low turbidity) is associated with higher MNDWI values, suggesting that stable or ponded water conditions allowed sediments to settle out. Thus, in areas where the modified water index signaled more distinct surface water presence, turbidity tended to decrease, reflecting sediment deposition and clearer water conditions.

While these correlation patterns help reveal internal consistency across indices, we acknowledge that their interpretation is limited by the lack of field-based validation data from the time of the 2003 incident. As explained in Section 3.1, no in-situ measurements were available due to the socio-political constraints of that period. Future work would benefit from integrating field surveys or drone-based water quality observations to confirm and calibrate satellite-derived inferences.

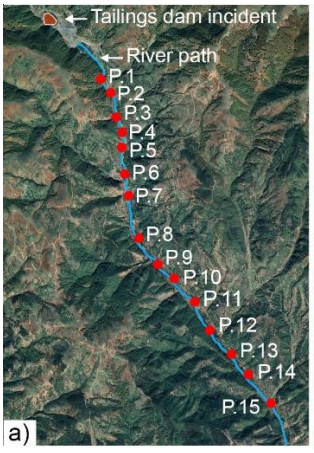

b)

Point ID	Latitude	Longitude	Distance (km)	NDVI	NDMI	NDWI	Turbidity	MNDWI
P.1	42.0949	22.5403	1.49	-0.0279	0.0226	0.0149	-0.0612	0.0320
P.2	42.0924	22.5424	1.82	-0.0466	-0.0092	0.0583	-0.0528	0.0475
P.3	42.0877	22.5441	2.33	-0.1123	-0.0608	0.1618	-0.0479	0.0998
P.4	42.0847	22.5455	2.67	-0.0654	-0.0792	0.0676	-0.0325	-0.0083
P.5	42.0823	22.5454	2.90	-0.0728	0.0357	0.0702	-0.0773	0.1008
P.6	42.0775	22.5460	3.39	-0.2076	-0.1511	0.1701	-0.0273	0.0608
P.7	42.0737	22.5466	3.80	-0.1536	-0.0886	0.1650	-0.0340	0.0846
P.8	42.0657	22.5495	4.71	-0.3331	-0.1659	0.3242	-0.0765	0.2409
P.9	42.0609	22.5545	5.37	-0.1579	-0.1496	0.1440	-0.0104	0.0293
P.10	42.0585	22.5581	5.74	-0.0903	-0.1341	0.0636	0.0144	-0.0225
P.11	42.0541	22.5637	6.37	-0.3653	-0.1347	0.4076	-0.0924	0.3054
P.12	42.0488	22.5674	7.03	-0.2424	-0.1313	0.2735	-0.0612	0.1952
P.13	42.0440	22.5726	7.71	0.0716	0.0980	-0.0112	-0.0468	0.0623
P.14	42.0407	22.5766	8.19	0.0527	-0.0279	-0.0378	-0.0014	-0.0710
P.15	42.0354	22.5824	8.94	-0.0385	-0.0396	0.0158	-0.0091	-0.0148

c)

Correlation Pairs	Pearson Correlation Coefficient
NDVI vs NDWI	-0.9742
NDMI vs MNDWI	-0.3519
NDWI vs Turbidity	-0.5701
NDMI vs NDWI	-0.7033
MNDWI vs Turbidity	-0.8242

Fig. 10. a) Sampled points along river path; b) Summary of environmental index differences for each sampling point, including latitude, longitude, and Euclidean distance (in km) from the tailings dam; c) Pearson correlation coefficients showing relationships between environmental indices at sampled points

4.4.3. Ecological and management implications

Thus, these point-based and correlation results underscore the multifaceted nature of tailings dam failure impacts. The strong negative correlation between NDVI and NDWI, for example, highlights a key management concern: higher water availability, while intuitively beneficial to some species, might prove extremely stressful to terrestrial vegetation adapted to permeable soil. Likewise, the cross-analysis of turbidity and MNDWI indicates how sediment-laden waters gradually become clear with particles forming a layer at the bottom in sluggish or areas with pooled water, creating a consequent shift in habitat supply to aquatic organisms.

4.4.4. Synthesis of point-based correlations and sampling patterns

By integrating in this manner, the fine-scaled sample with correlation analysis, we are provided with detailed insights into the correcting relationships that contribute to environmental alteration. These insights are crucial for developing context-specific mitigation measures, including drainage enhancements, to rehabilitative plantings that address multiple stressors simultaneously. In addition, these correlations suggest directions for future studies; that is, research on the processes connecting water dynamics, sediment regimes, and vegetation responses in post-disaster environments.

Altogether, the point-based, statistical analysis highlights the spatial heterogeneity of post-failure conditions and reveals key associations among environmental indices. The understanding of such local-scale patterns and relationships is useful in the development of appropriate, effective management strategies supporting post-tailings dam failure ecosystem rehabilitation and recovery.

4.5. Integrated analysis of zone-based Z-scores for environmental indices

While mean values and absolute differences are informative and give a clear indication of the degree and direction of environmental changes, they can be challenging to interpret in isolation. The mean differences in environmental indices and their corresponding global mean and standard deviation values, as illustrated in Fig. 11, were foundational for computing Z-scores across the zones. Therefore, to contextualise the noted changes into perspective, we determined the Z-scores for each environmental index difference in the three defined zones (Fig. 12). By normalising differences relative to the global mean and standard deviation values, Z-scores indicate whether certain areas exhibit changes that substantially deviate from broader baseline conditions.

4.5.1. Rationale for Z-score analysis

A Z-score transforms raw differences into standardised units and makes it easy to compare indices that may be on different scales and have different variances. Using the global mean and standard deviation values derived from Fig. 11, Z-scores enable consistent comparison across indices and zones. For example, a Z-score of +1 means that the observed difference is one standard deviation above the global mean, while a Z-score of –1 means one standard deviation below the global mean. Employing Z-scores is effective in identifying which zones exhibit high or low NDVI, NDMI, NDWI, turbidity, or MNDWI compared to the overall variability in the system.

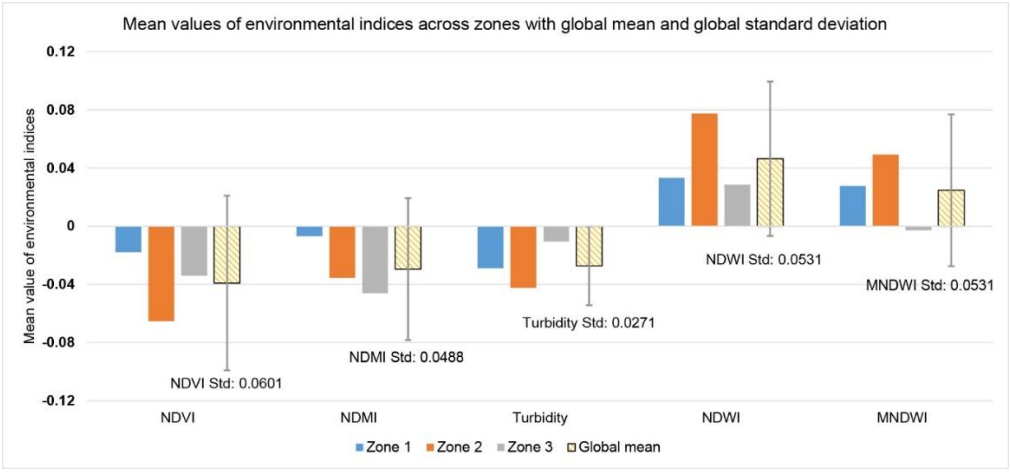

Fig. 11. Mean differences in environmental indices (NDVI, NDMI, turbidity, NDWI, and MNDWI) across zones with global mean and standard deviation: highlighting zone-specific and global variability in pre- and post-event environmental changes

4.5.2. Zone-by-zone comparisons

NDVI in Zone 1 showed a marginally positive Z-score, implying that vegetation conditions were not drastically different from the global average after the event (Fig. 12). However, NDMI in Zone 1 was positive, suggesting slightly enhanced soil moisture conditions relative to the worldwide context. For the same case, the NDWI and MNDWI values remained relatively stable, with NDWI showing slight negative deviations, indicating that localised water presence did not significantly differ from normal patterns. Turbidity values were also near baseline, suggesting that Zone 1's environmental conditions, despite being relatively close to the spill area, were not dramatically different from the overall environmental 'normal' recorded elsewhere in the study area. This could mean that flow conditions in the initial period enabled tailings to flow downstream rapidly, preventing sustained localised anomalies right in the vicinity of the source.

The Z-score profile at Zone 2 was more pronounced. A Z-score analysis for NDWI and MNDWI reflected a highly significant indication that this mid-distance zone contained more standing water or saturated surfaces than average, as the resulting values were above 0.5 (Fig. 12).

On the other hand, NDVI had a negative Z-score, which indicated below-average vegetation health compared to global conditions. Interestingly, the Z-score for turbidity in Zone 2 was a little above +0.5. This implies the existence of an environment where either hydrology or sediment loads co-occurred, creating conditions noticeably different from the norm. The decrease in vegetation cover, water availability and high turbidity in Zone 2 identified it as a "hotspot" from the tailings-induced environmental stress.

In Zone 3, several indices suggested more global-average conditions downstream. It is important here to observe that the Z-score of NDMI was negative (–0.3407), indicating that the amount of moisture in the soil of the sampled area was below the mean value observed system-wide (Fig. 12). At the same time, the NDWI values were slightly negative (–0.3350), and the MNDWI values were also negative (-0.5272). Turbidity had a positive Z-score (+0.6159), indicating some

remaining impact. These patterns suggest that by the time the tailings and, correspondingly, the impacts reached Zone 3, the sedimentation, dilution, and natural self-recovery brought the environmental conditions to levels similar to the natural system variability while retaining a certain after-shock effect. The slight variations here may be due to the fact that the tailings increasingly lost their impact downstream, confirming that downstream areas experienced less severe but clearly readable disturbances.

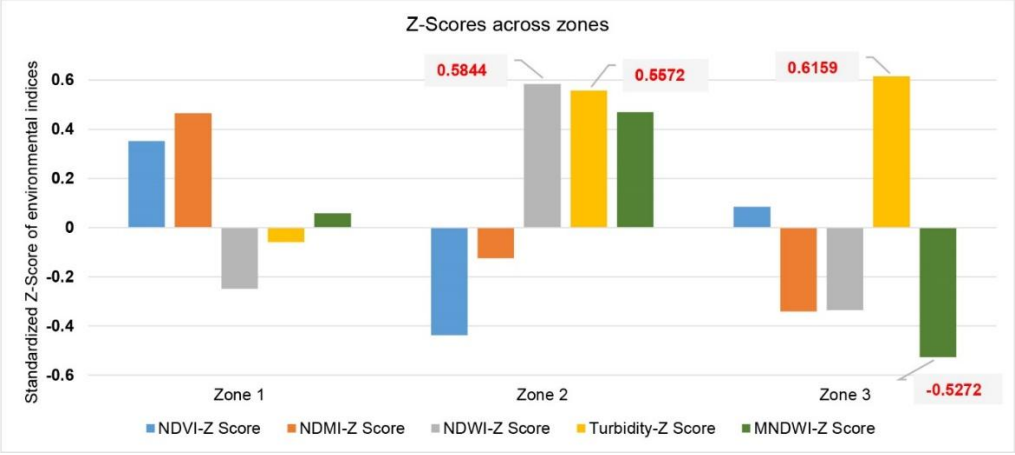

Fig. 12. Standardised Z-Scores for environmental indices (NDVI, NDMI, turbidity, NDWI, and MNDWI) across zones: highlighting variations in pre- and post-event changes relative to mean conditions

4.5.3. Ecological and management implications

Interpreting the environmental indices in standardised terms provides a perspective on the ecological implications of the spill. As seen from the outliers indicated by the particularly high Z-scores of NDWI, MNDWI and turbidity in Zone 2, this part of the river corridor was exposed to conditions that belong well outside the normal range, which may have caused stress to aquatic organisms, obstructed the recovery of vegetation cover and altered soil properties. Targeted interventions that can include sediment removal or channel stabilisation may be essential in these affected zones.

On the other hand, from the findings of this study, Zones 1 and 3 seem to represent more moderate or transient states of disturbance. Surprisingly, the standardised impact scores in Zone 1 are also notably moderate despite the fact that this location is nearest to the spill source, but again, probably owing to the quick dispersal of tailings. The values in Zone 3 displayed mild anomalies that showed effects moving downstream but were buffered by natural attenuation processes, reducing the severity.

4.5.4. Synthesis of zone-based Z-Score patterns

The Z-score analysis enhances the previous findings by measuring the extremity of observed changes. This supports the claim that the failure of the Sasa tailing dam did not produce a uniform

environmental response. However, truly segregated anthropogenic 'hotspots' emerged within Zone 2, standing out as an area with considerable disruption of hydrological and sediment conditions. Using such a multifaceted approach based on the absolute differences, the mean-based assessment and Z-scores provides a robust basis for targeted monitoring, remediation planning, and environmental management following mining-related disasters.

4.6. Comprehensive analysis of clustered environmental data

While the previous analyses looked at spatial gradients, differences between buffers, and point-based relationships, clustering allows for a more exploratory look at what may or may not be obvious from individual indices or simple correlations. Applying K-means to the set of sampled pixels, each characterised by changes in NDVI, NDMI, NDWI, MNDWI and turbidity, it was possible to isolate clusters of environmental reactions to the tailings dam failure. Compared to isolated metrics, these clusters present comprehensive profiles of ecosystem change that allow for a better understanding of post-disaster conditions.

4.6.1. Rationale for clustering analysis

Clustering allows us to group pixels with similar combinations of index differences into distinct classes. Unlike previous methods that focus on a single parameter, such as vegetation health, or rely on pairwise correlations, this approach simultaneously integrates all the indices. Consequently, each cluster can best be described as a coherent environmental 'type' that emerges naturally from the data, illustrating how various indicators of vegetation stress, soil moisture change, water presence, and turbidity collectively define particular post-disturbance states.

Fig. 13a-d shows scatterplots of index differences (pre- and post-event) (NDMI vs. MNDWI, NDWI vs. Turbidity, NDVI vs. NDWI, NDVI vs. NDMI) for several index pairs, and each pixel

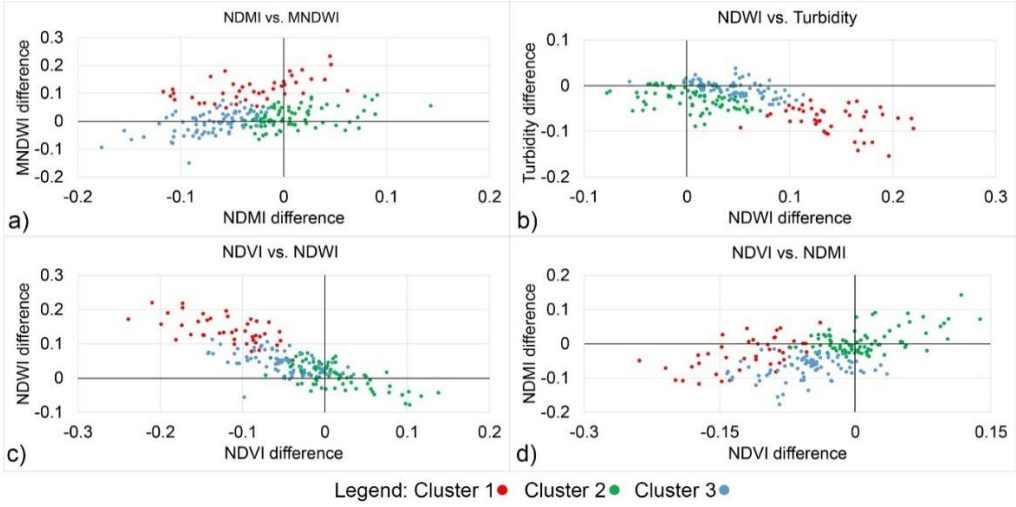

Fig. 13. Cluster-based analysis of environmental index differences (pre- and post-event) across zones: (a) NDMI vs. MNDWI; (b) NDWI vs. Turbidity; (c) NDWI vs. NDVI; (d) NDVI vs. NDMI

is colored according to the cluster to which it belongs. These cluster assignments come out of a high-dimensional space, making use of two-dimensional projections to help interpret their underlying characteristics.

The red cluster points (cluster 1) lie in the areas of the scatterplots representing higher moisture and water-related indices (elevated NDMI and MNDWI), yet their vegetation-related values (NDVI) often do not show enhancements and, in some cases, are even slightly reduced. In other words, this cluster may be indicative of regions where there is an excess of moisture or standing water, due to altered flow regimes by tailings that could have limited vegetation regeneration or induced stress. The presence of water could contain settled sediment that could lead to moderate turbidity changes, but the conditions were still unfavourable for the growth of plants. Therefore, we can define cluster 1 as zones with a high moisture level and an ecologically constrained environment.

The green cluster (Cluster 2) frequently signifies mid-range position in the index difference space, suggesting a more balanced or transitional state. These pixels could correspond to areas where the influence of the tailings impact was present but not extreme. The vegetation health decreased only with moderate values, soil moisture changes were noticeable but not extreme and water-related indices shifted slightly. Cluster 2 may reflect environments that are either partially buffered from the most intense disturbances or on a trajectory toward gradual ecological stabilisation. These landscapes may heal incrementally as sedimentation settles and vegetation re-establishes itself.

It is with the blue cluster (Cluster 3) that its prevailing conditions correspond to those of reduced vegetation health (negative NDVI differences), and lower availability of soil moisture (negative NDMI differences), accompanied by comparatively stable or only slightly shifting water indices. This cluster may be associated with areas where vegetation regeneration was poor, possibly due to residual sediment contamination, nutrient depletion, or physical substrate changes. It indicates that lower moisture levels could intensify pressure on the plants, and even if water availability is not significantly changed, the absence of vegetation cover points to acute long-term environmental problems. Consequently, cluster 3 reveals that areas observed post-event that are drier and less vegetated are areas that continue to experience persistent ecological deterioration.

4.6.2. Ecological and management implications

Certain sites intensified to a wet and less vegetated environment (Cluster 1), others fluctuated at a moderate level of disturbance (Cluster 2), and some transitioned to a dry and degraded state (Cluster 3). Understanding these patterns enables more targeted interventions. For example, the process of conservation and rehabilitation in the areas of Cluster 1 can address the possibilities of drainage or stabilisation of water levels for vegetation regeneration. In Cluster 3 zones, the possibilities of ecological remediation include such measures as soil addition, planting of vegetation cover or applications of erosion control.

4.6.3. Synthesis of clustered environmental patterns

The presented clustering analysis underlines the complexity and heterogeneity of post-failure landscapes. Each cluster describes a unique environmental role that occurs through interactions between hydrological fluctuations, sedimentation, and vegetation stress. These subtler data-driven insights are built upon earlier findings, providing piece-by-piece, targeted guidance for the de-

velopment of complex restoration ecosystems to help meet the needs of each of the identified clusters. In doing so, we shift away from simplistic "before-and-after" narratives and enhance possibilities for practical interpretations of ecosystem changes in relation to mine-related disasters.

4.7. Analysis of vegetation and moisture changes in relation to topographic factors

Topographic variables such as distance downstream and elevation can significantly control ecological factors like the distribution of vegetation, the ability of soil to retain moisture and sediment transport dynamics. To be able to assess whether these broader landscape gradients shaped the environmental responses observed after the Sasa tailing dam failure, we examined the relationship between environmental index differences in NDVI, NDMI, and Turbidity and two key topographic parameters, which include the distance from the spill incident along the river corridor and elevation.

Figs. 14a and 14c show scatter plots of NDVI and NDMI differences against distance and reveal minimal or no strong linear relationship. For NDVI, the coefficient of determination $R^2 = 0.0062$, indicating an extremely weak relationship. NDMI is only slightly better ($R^2 = 0.098$), again indicating that there is a general trend that distance does not systematically explain variation in the change of soil moisture across the study area.

These results suggest that patterns and changes in vegetation and moisture following the failure of the dam are governed more by local factors such as the distribution of sediment or microhabitat variability. Although one might expect contamination or sediment loads to disperse and dilute with distance, the weak correlations suggest that non-uniform deposition, channel geometry or other factors provided the decisive role in determining local environmental outcomes.

Similarly, the plots corresponding to differences in NDVI and turbidity with respect to elevation (Figs. 14b, 14d) have very low R^2 values, 0.0218 for NDVI and 0.0336 for turbidity. These

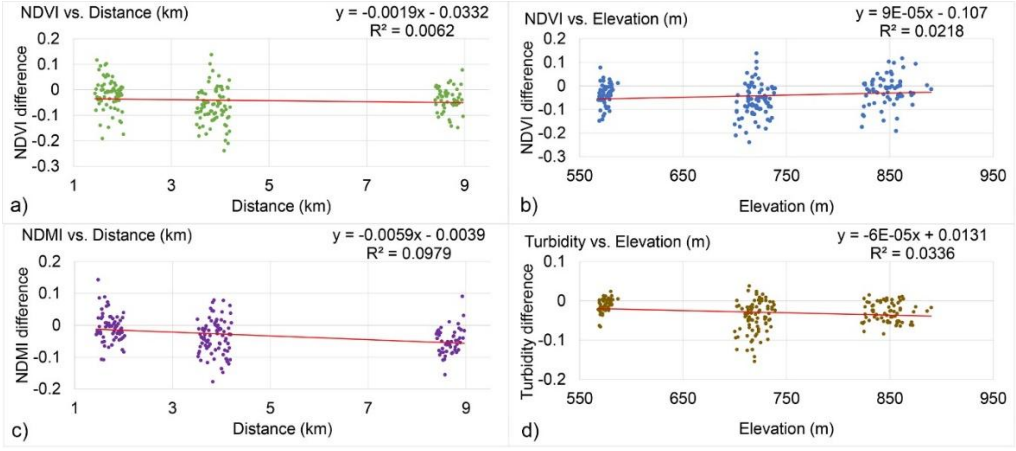

Fig. 14. Linear relationships between environmental index differences and topographic factors: (a) NDVI difference vs. distance (km); (b) NDVI difference vs. elevation (m); (c) NDMI difference vs. distance (km); (d) Turbidity difference vs. elevation (m)

values indicate that elevation alone did not have a significant effect on the degree of vegetation recovery or sediment settling patterns.

If elevation gradients were crucial drivers, more straightforward patterns could be identified, such as increased sediment deposition or higher vegetation stress at certain elevations, but no such patterns emerged.

The absence of a correlation may be an indication that although topography acts as a determinant of long-term river morphology and sediment distribution, the circumstances that prevailed within the immediate aftermath of the tailings dam failure were more influenced by site-specific localised factors. Such factors could be in the form of temporal and spatial variability in rainfall patterns and impacts, the physical and mechanical characteristics of the tailings material, localised flow obstructions or intervention activities after the spill.

Therefore, in the absence of a strong linear relationship between the topographic variables and the environmental indices, the context of the landscape remains important. Instead, it draws attention to a detailed range of post-disaster landscapes, where general characteristics such as elevation or longitudinal position along a river fail to capture the complex relationships of site-specific conditions. Previous sections showed how the effects of the tailings spill were highly variable and often clustered, reflecting localised processes rather than simple, large-scale patterns.

In regard to the management approach, this result points out that remediation efforts cannot rely solely on broad assumptions about how impacts dissipate downstream or change at different elevations. Rather, precise, site-specific assessments are still necessary. Fine-scale intervention strategies, developed by high-resolution remote sensing and ground-based evaluations, are likely to be more effective than topography-guided approaches.

4.7.1. Synthesis of vegetation and moisture-topography relationships

Overall, the findings indicate that despite topography influencing ecosystems, it was not the dominant factor shaping the post-event vegetation health, soil moisture, and sediment condition following the Sasa tailing dam incident. A number of these short-term environmental responses seem to have been influenced by sediment movements and hydrological disruptions rather than broad-scale elevation or distance gradients. These observations support the argument in favour of integrative and multiple-scale approaches for environmental assessment that also frame site-specific information with broader contextual understanding of the consequences of tailings dam failures.

4.8. Spatial analysis of Cumulative Impact Scores (CIS) and index-based environmental stress

Environmental degradation resulting from the Sasa tailings dam failure was assessed by analysing the CIS and individual indices (NDVI and NDWI differences) across three zones (Fig. 15a). Statistical analysis of the CIS revealed a mean value of 0.0049, with a standard deviation of 0.0167, indicating moderate variation in environmental stress across the sampled zones (Fig. 15b). The CIS varied from a minimum of –0.074 to a maximum of 0.0525, indicating variability in impact levels.

Zone 1 presented regional point clusters with high cumulative impact values, especially in the regions that were affected by the spill. NDVI differences in this zone revealed areas of severe

vegetation loss that complement the higher CIS values. Similarly, differences in the NDWI pointed out areas that experienced moisture depletion, which could be attributable to the interruption of the hydrological flows caused by the spill. Taken together, these results highlight the elevated levels of ecological pressure in specific parts of Zone 1.

Zone 2 exhibited a similar pattern, with a high concentration of CIS values in specific areas. The changes of NDVI revealed moderate to high levels of vegetation loss, and these were more pronounced in the middle portion of the zone. The differences in NDWI values pointed to localised moisture retention, which could imply the presence of accumulation or waterlogging in certain areas. This pattern aligns with the downstream spreading of the spill and its impact on vegetation and water systems.

Zone 3 was identified as having relatively moderate CIS compared to Zones 1 and 2. The results of the NDVI differences in this zone were not very alarming, indicating areas with moderate vegetation health. NDWI differences were consistent with balanced moisture levels across the zone, indicating that Zone 3 was relatively less affected by the hydrological changes.

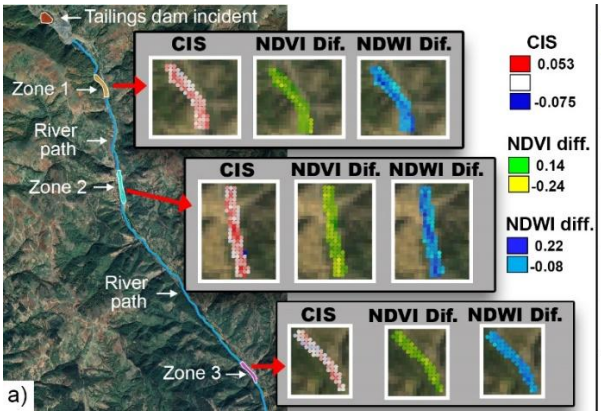

Statistic	Value
Maximum	0.0525
Mean	0.0049
Minimum	-0.074
Sample Standard Deviation	0.0167
Sample Variance	0.0002
Sum	0.9812
Sum of Squares	0.0601
Total Count of points	199
Total Standard Deviation	0.0166
Total Variance	0.0002
Weighted Sum	0.9812

(b)

Fig. 15. (a) Spatial distribution of CIS, NDVI differences, and NDWI differences across zones 1, 2, and 3; (b) Statistical summary of CIS values highlighting key metrics including mean, standard deviation, and range

The visualizations regarding the CIS and individual indices added value to the spatial interpretation of environmental stress. The CIS heatmaps, with the blue to red gradients successfully distinguished low, moderate, and high impact zones (Fig. 15a). Likewise, the green-yellow NDVI gradients enhanced the vegetation degradation aspect, while the cyan-blue NDWI gradients highlighted differences in the moisture conditions. These visualization tools were helpful in pointing at critical zones and in overall assessment of the effects based upon vegetation, moisture, and water quality.

4.8.1. Synthesis of spatial patterns in environmental stress

The assessment of the CIS, as well as the assessment of individual indices, proves that the failure of the tailings dam had spatially varied consequences. Based on higher CIS values and associated vegetation and moisture impacts, zones 1 and 2 were identified as critical areas for intervention. Zone 3 experienced relatively low changes, but there were localised impacts that

need to be continually monitored to ensure ecological rehabilitation. This integrative approach, combining statistical, spatial, and visual analyses, provides a comprehensive framework for understanding and addressing the environmental effects of mining-related disasters.

4.9. Validation of index changes

TABLE 1 presents findings from the sensitivity analysis conducted for the indices within a 10 m buffer zone along the river path. The data from 273 valid sampled pixels showed that both NDVI and NDMI registered negative mean differences (i.e., declines in vegetation health and moisture) – while NDWI and MNDWI exhibited notable increases, indicating greater water presence post-event. The measured turbidity levels within the buffer zones showed no statistically relevant alterations between pre-event and post-event dates.

TABLE 1

Statistical sensitivity analysis of environmental index differences (pre- and post-event) within the 10 m buffer zone along the river path

Index	Mean Difference	Standard Deviation	Shapiro-Wilk p-value	Test Used	*p*-value	Significant
NDVI	−0.085	0.099	<0.001	Wilcoxon Signed-Rank Test	<0.001	Yes
NDMI	−0.044	0.075	<0.001	Wilcoxon Signed-Rank Test	<0.001	Yes
NDWI	+0.089	0.093	<0.001	Wilcoxon Signed-Rank Test	<0.001	Yes
MNDWI	+0.058	0.078	0.000003	Wilcoxon Signed-Rank Test	<0.001	Yes
Turbidity	−0.004	0.102	0.0127	Wilcoxon Signed-Rank Test	0.296	No

The data presented in TABLE 1 shows mean differences, standard deviations, and Wilcoxon signed-rank test results from 273 pixel measurements ($n = 273$ pixels) for each index. All statistically significant changes ($p < 0.05$) are highlighted.

The significantly negative NDVI/NDMI shifts show actual vegetation stress combined with moisture stress near the riverbed, thus strengthening research findings about immediate ecological impacts in the area. As signalled by statistically significant positive values in NDWI/MNDWI data, there is a notion that tailings material may have impeded drainage or encouraged localised water accumulation.

Although turbidity index changes were not showing a statistical change within the 10 m buffer zone ($p = 0.296$), the index still showed a consistent negative trend across the broader corridor. As illustrated in Fig. 8, the mean turbidity index declined progressively in both the 25 m and 50 m buffer zones. Furthermore, Fig. 9 highlights that Zone 2, located directly downstream of the tailings failure, exhibited the most pronounced decrease in turbidity (mean difference = −0.0424), suggesting localised sediment deposition.

The appearance of the observed pattern may be attributed to two main factors: (i) the post-event image was acquired 18 days after the incident, providing time for suspended sediment to settle or be flushed downstream, and (ii) the turbidity index used in this study is a surface reflectance-based proxy, which may lack sensitivity to detect short-lived or subsurface sediment plumes. Additionally, the relatively high variability in turbidity differences across sample points likely contributed to the lack of statistical significance in the 10 m buffer zone despite spatial evidence of change.

Taken together, these results suggest that while no statistically significant turbidity spike was captured in our primary test area, sediment transport and deposition processes likely occurred immediately after the tailings dam failure.

5. Conclusion

This research illustrates the value and significance of a comprehensive, multi-index remote sensing framework for evaluating the complex environmental impacts resulting from a tailings dam failure. Concentrating on the 2003 Sasa tailing dam incident in N. Macedonia – a location that has been underrepresented in existing research – we demonstrate how employing complementary spectral indices (NDVI, NDMI, NDWI, MNDWI, and a turbidity indicator) can uncover detailed spatial variations of ecological effects. Through the examination of shifts in vegetation health, soil moisture levels, water presence, and sediment load at the same spatial scales, while applying diverse analytical methods, this study provides a multi-perspective view of post-disaster landscape dynamics.

The results reveal that the surrounding river corridor was the most impacted and affected by the diverse types of disturbance, such as vegetation stress, changing soil moisture conditions, persistent standing water, and elevated turbidity. From the river channel, the disturbances decreased with distance, and these impacts were less pronounced and had unique features in defined zones along the river pathway. At some sites, notably those at intermediate distances from the incident, conditions took on characteristics of what could be called 'environmental hotspots,' displaying favourable conditions for both sedimentation and water accumulation that limited vegetation recovery. The spatial heterogeneity was further analysed by the clustering analysis, which grouped the pixels with similar integrated responses, indicating a rather obvious fact that there cannot be a single index or simple metric that could adequately describe post-disaster conditions.

Statistical approaches, including Z-score and correlation analyses, provided a basis for interpreting the changes in indices from the baseline conditions. These analyses supported our hypothesis that some areas exhibited substantial, statistically significant outliers, whereas others showed less marked deviations from the system averages. Equally important, the weak relationships that were established between the topographic gradients and environmental response imply that the site-specific conditions, rather than the general elevation or simple downstream distance effects, were the main determinants of short-term ecological dynamics. These findings challenge the assumption that large-scale landscape gradients alone can explain environmental outcomes following tailings dam failures, establishing the importance of site-specific factors and remediation strategies.

This comprehensive assessment offers key features relevant to both environmental science and disaster management. Thus, by recording the extent to which vegetation, soil moisture, and water-related parameters respond to contamination events, the work provides usable information on how to restore the impacted areas. This methodology allows practitioners to isolate the areas that require the most attention, for instance, to improve drainage in the areas saturated with water, to stabilise sediments in the sections that can provoke increased water turbidity, or to replant vegetation in areas where stress effects are the most significant.

Apart from this case study, the outlines of the methodological framework and the analytical strategy described here can be applied to other mining regions and other types of environmental

emergencies. As climate variability and resource extraction pressures continue to increase, the frequency of tailings dam failures and similar disturbances may also rise. Through setting up a methodologically sound, replicable, and integrative remote sensing approach, this research provides a baseline for more proactive, evidence-based management practices. Finally, enhanced knowledge of environmental resilience, vulnerability, and post-mining recovery will strengthen policy solutions aimed at protecting ecosystems and communities exposed to the dangers of mining-related environmental disasters.

Acknowledgment

The authors would like to express their sincere gratitude to Goce Delcev University, Stip, North Macedonia, for providing financial support for the publication of this paper. Additionally, the authors would like to thank the editor and the anonymous reviewers for their valuable comments and suggestions, which have significantly contributed to improving the quality and clarity of this work.

References

[1] D. Cheng, Y. Cui, Z. Li, J. Iqbal, Watch Out for the Tailings Pond, a Sharp Edge Hanging over Our Heads: Lessons Learned and Perceptions from the Brumadinho Tailings Dam Failure Disaster. Remote Sens. **13** (9), 1775 (2021). DOI: https://doi.org/10.3390/rs13091775

[2] D. Kossoff, W.E. Dubbin, M. Alfredsson, S.J. Edwards, M.G. Macklin, K.A. Hudson-Edwards, Mine tailings dams: Characteristics, failure, environmental impacts, and remediation. Appl. Geochem. **51**, 229-45 (2014). DOI: https://doi.org/10.1016/j.apgeochem.2014.09.010

[3] C.Y. Omachi, S.M.O. Siani, F.M. Chagas, M.L. Mascagni, M. Cordeiro, G.D. Garcia, et al., Atlantic Forest loss caused by the world's largest tailing dam collapse (Fundão Dam, Mariana, Brazil). Remote Sens. Appl.: Soc. Environ. **12**, 30-4 (2018). DOI: https://doi.org/10.1016/j.rsase.2018.08.003

[4] N. Rudorff, C.M. Rudorff, M. Kampel, G. Ortiz, Remote sensing monitoring of the impact of a major mining wastewater disaster on the turbidity of the Doce River plume off the eastern Brazilian coast. Int. Soc. Photogramme. **145**, 349-61 (2018). DOI: https://doi.org/10.1016/j.isprsjprs.2018.02.013

[5] L.H. Silva Rotta, E. Alcântara, E. Park, R.G. Negri, Y.N. Lin, N. Bernardo, et al., The 2019 Brumadinho tailings dam collapse: Possible cause and impacts of the worst human and environmental disaster in Brazil. Int. J. Appl. Earth. Obs. **90**, 102119 (2020). DOI: https://doi.org/10.1016/j.jag.2020.102119

[6] U.R.V. Aires, B.S.M. Santos, C.D. Coelho, D.D. Da Silva, M.L. Calijuri, Changes in land use and land cover as a result of the failure of a mining tailings dam in Mariana, MG, Brazil. Land. Use. Policy. **70**, 63-70 (2018). DOI: https://doi.org/10.1016/j.landusepol.2017.10.026

[7] D.B.D.S. Teixeira, M.F. Veloso, F.L.V. Ferreira, J.M. Gleriani, C.H. Do Amaral, Spectro-temporal analysis of the Paraopeba River water after the tailings dam burst of the Córrego do Feijão mine, in Brumadinho, Brazil. Environ. Monit. Assess. **193** (7), 435 (2021). DOI: https://doi.org/10.1007/s10661-021-09218-4

[8] F. Thompson, B.C. De Oliveira, M.C. Cordeiro, B.P. Masi, T.P. Rangel, P. Paz, et al., Severe impacts of the Brumadinho dam failure (Minas Gerais, Brazil) on the water quality of the Paraopeba River. Sci. Total. Environ. **705**, 135914 (2020). DOI: https://doi.org/10.1016/j.scitotenv.2019.135914

[9] C. Cacciuttolo, D. Cano, Spatial and Temporal Study of Supernatant Process Water Pond in Tailings Storage Facilities: Use of Remote Sensing Techniques for Preventing Mine Tailings Dam Failures. Sustainability-Basel. **15** (6), 4984 (2023). DOI: https://doi.org/10.3390/su15064984

[10] S.M. Ouellet, J. Dettmer, G. Olivier, T. DeWit, M. Lato, Advanced monitoring of tailings dam performance using seismic noise and stress models. Comm. Earth Environ. **3** (1), 301 (2022). DOI: https://doi.org/10.1038/s43247-022-00629-w

[11] A.P.D. Souza, P.E. Teodoro, L.P.R. Teodoro, A.C. Taveira, J.F. De Oliveira-Júnior, J.L. Della-Silva, et al., Application of remote sensing in environmental impact assessment: a case study of dam rupture in Brumadinho, Minas Gerais, Brazil. Environ. Monit. Assess. **193** (9), 606 (2021). DOI: https://doi.org/10.1007/s10661-021-09417-z

[12] M. Zare, F. Nasategay, J.A. Gomez, A. Moayedi Far, J. Sattarvand, A Review of Tailings Dam Safety Monitoring Guidelines and Systems. Mineral-Basel. **14** (6), 551 (2024). DOI: https://doi.org/10.3390/min14060551

[13] M.M. Harb, F. Dell'Acqua, Remote Sensing in Multirisk Assessment: Improving disaster preparedness. IEEE. Geosci. Remote. M. **5** (1), 53-65 (2017). DOI: https://doi.org/10.1109/MGRS.2016.2625100

[14] C. Huyck, E. Verrucci, J. Bevington, Remote Sensing for Disaster Response : A Rapid, Image-Based Perspective. Earthq. Hazard Risk Disasters. 1-24 (2014). DOI: https://doi.org/10.1016/B978-0-12-394848-9.00001-8

[15] S. Kumari, S. Agarwal, N.K. Agrawal, A. Agarwal, M.C. Garg, A Comprehensive Review of Remote Sensing Technologies for Improved Geological Disaster Management. Geol. J. **60** (1), 223-35 (2025). DOI: https://doi.org/10.1002/gj.5072

[16] P.S. Showalter, Remote sensing's use in disaster research: a review. Disaster. Prev. Manag. **10** (1), 21-9 (2001). DOI: https://doi.org/10.1108/09653560110381796

[17] L. Ammirati, R. Chirico, D. Di Martire, N. Mondillo, Application of Multispectral Remote Sensing for Mapping Flood-Affected Zones in the Brumadinho Mining District (Minas Gerais, Brasil). Remote Sens. **14** (6), 1501 (2022). DOI: https://doi.org/10.3390/rs14061501

[18] S. Grebby, A. Sowter, J. Gluyas, D. Toll, D. Gee, A. Athab, et al., Advanced analysis of satellite data reveals ground deformation precursors to the Brumadinho Tailings Dam collapse. Commun. Earth Environ. **2** (1), 2 (2021). DOI: https://doi.org/10.1038/s43247-020-00079-2

[19] N.M. Rana, K.B. Delaney, S.G. Evans, E. Deane, A. Small, D.A.M. Adria, et al., Application of Sentinel-1 InSAR to monitor tailings dams and predict geotechnical instability: practical considerations based on case study insights. B. Eng. Geol. Environ. **83** (5), 204 (2024). DOI: https://doi.org/10.1007/s10064-024-03680-3

[20] P.L.B. Crioni, E.H. Teramoto, H.K. Chang, Monitoring river turbidity after a mine tailing dam failure using an empirical model derived from Sentinel-2 imagery. An. Acad. Bras. Cienc. **95** (1), e20220177 (2023). DOI: https://doi.org/10.1590/0001-3765202320220177

[21] C.R.M. Filho, R.F. Do Valle Junior, M.M.A.P. De Melo Silva, R.G. Mendes, G. De Souza Rolim, T.C.T. Pissarra, et al., The Accuracy of Land Use and Cover Mapping across Time in Environmental Disaster Zones: The Case of the B1 Tailings Dam Rupture in Brumadinho, Brazil. Sustainability-Basel. **15** (8), 6949 (2023). DOI: https://doi.org/10.3390/su15086949

[22] P. Vrhovnik, N. Rogan Šmuc, T. Dolenec, T. Serafimovsi, G. Tasev, M. Dolenec, Geochemical investigation of Sasa tailings dam material and its influence on the Lake Kalimanci surficial sediments (Republic of Macedonia) – preliminary study. Geologija **53** (2), 169-76 (2011). DOI: https://doi.org/10.5474/geologija.2011.013

[23] P. Vrhovnik, N.R. Šmuc, T. Dolenec, T. Serafimovski, M. Dolenec, An evaluation of trace metal distribution and environmental risk in sediments from Lake Kalimanci (FYR Macedonia). Environ. Earth. Sci. **70** (2), 761-75 (2013). DOI: https://doi.org/10.1007/s12665-012-2166-1

[24] R. Sangeetham, N. Reddy S, A Review On Google Earth Engine: An Open Access Cloud Analysis Platform For Planetary Scale Satellite Data. E3S. Web. Conf. **591**, 09011 (2024). DOI: https://doi.org/10.1051/e3sconf/202459109011

[25] Q. Zhao, L. Yu, X. Li, D. Peng, Y. Zhang, P. Gong, Progress and Trends in the Application of Google Earth and Google Earth Engine. Remote Sens. **13** (18), 3778 (2021). DOI: https://doi.org/10.3390/rs13183778

[26] M. Hemati, M. Hasanlou, M. Mahdianpari, F. Mohammadimanesh, A Systematic Review of Landsat Data for Change Detection Applications: 50 Years of Monitoring the Earth. Remote Sens. **13** (15), 2869 (2021). DOI: https://doi.org/10.3390/rs13152869

[27] V. Kharat, S. Khatdeo, H. Kothe, R. Kshirsagar, M. Dixit, M.S. Balan, Atmospheric Image Correction and Removal of Cloud Cover for Satellite Images. 2023 Int. Conf. Sustain. Comput. Smart Syst. 1711-8 (2023). DOI: https://doi.org/10.1109/icscss57650.2023.10169542

[28] G. Chander, B.L. Markham, J.A. Barsi, Revised Landsat-5 Thematic Mapper Radiometric Calibration. IEEE Geosci. Remote S. **4** (3), 490-4 (2007). DOI: https://doi.org/10.1109/lgrs.2007.898285

[29] B. cai Gao, NDWI – A normalized difference water index for remote sensing of vegetation liquid water from space. Remote Sens. Environ. **58** (3), 257-66 (1996). DOI: https://doi.org/10.1016/S0034-4257(96)00067-3

[30] S.K. McFeeters, The use of the Normalized Difference Water Index (NDWI) in the delineation of open water features. Int. J. Remote Sens. **17** (7), 1425-32 (1996). DOI: https://doi.org/10.1080/01431169608948714

[31] S. Szabó, Z. Gácsi, B. Balázs, Specific features of NDVI, NDWI and MNDWI as reflected in land cover categories. Landsc. Environ. **10** (3-4), 194-202 (2016). DOI: https://doi.org/10.21120/LE/10/3-4/13

[32] Y. Wang, F. Huang, Y. Wei, Water body extraction from LANDSAT ETM+ image using MNDWI and K-T transformation. 2013 21st Int. Conf. Geoinf. 1-5 (2013). DOI: https://doi.org/10.1109/geoinformatics.2013.6626162

[33] X. Xiao, D. Hollinger, J. Aber, M. Goltz, E.A. Davidson, Q. Zhang, et al., Satellite-based modeling of gross primary production in an evergreen needleleaf forest. Remote Sens. Environ. **89** (4), 519-34 (2004). DOI: https://doi.org/10.1016/j.rse.2003.11.008

[34] D. Browning, C. Steele, Vegetation Index Differencing for Broad-Scale Assessment of Productivity Under Prolonged Drought and Sequential High Rainfall Conditions. Remote Sens. **5** (1), 327-41 (2013). DOI: https://doi.org/10.3390/rs5010327

[35] T.L. Swetnam, S.R. Yool, S. Roy, D.A. Falk, On the Use of Standardized Multi-Temporal Indices for Monitoring Disturbance and Ecosystem Moisture Stress across Multiple Earth Observation Systems in the Google Earth Engine. Remote Sens. **13** (8), 1448 (2021). DOI: https://doi.org/10.3390/rs13081448

[36] P. Lemenkova, O. Debeir, R Libraries for Remote Sensing Data Classification by K-Means Clustering and NDVI Computation in Congo River Basin, DRC. Appl. Sci-Basel. **12** (24), 12554 (2022). DOI: https://doi.org/10.3390/app122412554

[37] A. Mimenbayeva, S. Artykbayev, R. Suleimenova, G. Abdygalikova, A. Naizagarayeva, A. Ismailova, Determination of the number of clusters of normalized vegetation indices using the k-means algorithm. East.-Eur. J. Enterp. Technol. **5** (2 (125)), 42-55 (2023). DOI: https://doi.org/10.15587/1729-4061.2023.290129

[38] A. Nelson, T. Oberthür, S. Cook, Multi-scale correlations between topography and vegetation in a hillside catchment of Honduras. Int. J. Geogr. Inf. Sci. **21** (2), 145-74 (2007). DOI: https://doi.org/10.1080/13658810600852263

[39] N.A.S. Sampaio, F.C. Mazza, S.S.S.D. Siqueira, J.E. Miranda Junior, J.V.D.S. Moutinho, L.D.O. Pacífico, Applications of Correlation Analysis in Environmental Problems. Rev. Gest. Soc. Ambient. **18** (3), e04925 (2024). DOI: http://dx.doi.org/10.24857/rgsa.v18n3-085

[40] D.W. Clow, L. Nanus, B. Huggett, Use of regression-based models to map sensitivity of aquatic resources to atmospheric deposition in Yosemite National Park, USA. Water Resour. Res. **46** (9), 2009WR008316 (2010). DOI: https://doi.org/10.1029/2009WR008316

[41] G. Pickup, V.H. Chewings, Correlations between dem-derived topographic indices and remotely-sensed vegetation cover in rangelands. Earth Surf. Proc. Land. **21** (6), 517-29 (1996). DOI: https://doi.org/10.1002/(SICI)1096-9837(199606)21:6<517::AID-ESP609>3.0.CO;2-N

[42] B. Pratt, H. Chang, Effects of land cover, topography, and built structure on seasonal water quality at multiple spatial scales. J. Hazard. Mater. **209-210**, 48-58 (2012). DOI: https://doi.org/10.1016/j.jhazmat.2011.12.068

[43] G.C. Avena, C. Ricotta, F. Volpe, The influence of principal component analysis on the spatial structure of a multispectral dataset. Int. J. Remote Sens. **20** (17), 3367-76 (1999). DOI: https://doi.org/10.1080/014311699211381

[44] J. Estornell, J.M. Martí-Gavliá, M.T. Sebastiá, J. Mengual, Principal component analysis applied to remote sensing. Model. Sci. Educ. Learn. **6**, 2 (2013). DOI: https://doi.org/10.4995/msel.2013.1905